

# Charge- and anion-orderings in the quasi-one-dimensional organic conductor (TMTTF)<sub>2</sub>NO<sub>3</sub>

Olga Iakutkina, Lena Nadine Majer, Guilherme Gorgen Lesseux, Gabriele Untereiner, and Martin Dressel

*1. Physikalisches Institut, Universität Stuttgart, 70569 Stuttgart, Germany*

(Dated: April 23, 2021)

The quasi-one-dimensional organic conductors (TMTTF)<sub>2</sub>X with non-centrosymmetric anions commonly undergo charge- and anion-order transitions upon cooling. While for compounds with tetrahedral anions ( $X = \text{BF}_4^-$ ,  $\text{ReO}_4^-$ , and  $\text{ClO}_4^-$ ) the charge-ordered phase is rather well understood, the situation is less clear in the case of planar triangular anions, such as (TMTTF)<sub>2</sub>NO<sub>3</sub>. Here we explore the electronic and structural transitions by transport experiments, optical and magnetic spectroscopy. This way we analyze the temperature dependence of the charge imbalance  $2\delta$  and an activated behavior of  $\rho(T)$  with  $\Delta_{\text{CO}} \approx 530$  K below  $T_{\text{CO}} = 250$  K. Since (TMTTF)<sub>2</sub>NO<sub>3</sub> follows the universal relation between charge imbalance  $2\delta$  and size of the gap  $\Delta_{\text{CO}}$ , our findings suggest that charge order is determined by TMTTF stacks with little influence of the anions. Clear signatures of anion ordering are detected at  $T_{\text{AO}} = 50$  K. The tetramerization affects the dc transport, the vibrational features of donors and acceptors, and leads to formation of spin singlets.

PACS numbers: 74.70.Kn, 71.30.+h, 75.25.Dk, 74.25.Gz

## I. INTRODUCTION

In low-dimensional electron systems the influence of electronic correlations becomes more pronounced and may govern the effects of the crystal lattice [1, 2]. A prime example is given by the quasi-one-dimensional Fabre salts (TMTTF)<sub>2</sub>X, where TMTTF stands for tetramethyltetratiofulvalene and X is a monovalent anion. By stoichiometry these systems possess three-quarter-filled conduction bands but dimerization leads to effectively half-filling. Although they are supposed to be metals according to their band structure, electron-electron interaction leads to charge localization. Furthermore, different broken-symmetry ground states can be realized depending on the subtle interplay of charge, spin, and lattice degrees of freedom [3–7].

In (TMTTF)<sub>2</sub>X salts with octahedral anions ( $X = \text{PF}_6^-$ ,  $\text{AsF}_6^-$ ,  $\text{SbF}_6^-$ , and  $\text{TaF}_6^-$ ) charge order (CO) was extensively investigated by several methods [8–12]. A regular 1010 charge pattern develops along the molecular stacking axis  $a$  below the transition temperature  $T_{\text{CO}}$ . For non-centrosymmetric anions ( $X = \text{BF}_4^-$ ,  $\text{ReO}_4^-$ , and  $\text{ClO}_4^-$ ) situation is more complicated because – in addition to the CO phase transition – the anion may order (AO) in an alternating fashion at low temperatures, which leads to a tetramerization of the donor molecules [13–16] and doubling of the charge pattern to alternating sequence 0110 below  $T_{\text{AO}}$ . Despite the different anion size, for all these compounds a universal relation between charge imbalance  $2\delta$ , ordering temperature  $T_{\text{CO}}$  and charge gap  $\Delta_{\text{CO}}$  was revealed [17], which implies that the CO state is intrinsic for the TMTTF stacks and mainly determined by a competition between the inter-site Coulomb repulsion  $V$  and the bandwidth  $W$ .

So far, the detailed investigation were confined to (TMTTF)<sub>2</sub>X salts with tetrahedral anions, while other

symmetries were considered only incidentally. For (TMTTF)<sub>2</sub>SCN with linear anions, CO coincides with the ordering of the non-centrosymmetric anions [12]. The situation is even more complex in the case of  $X = \text{NO}_3^-$ , where the planar anions have trigonal symmetry. For decades it is discussed in the community whether or not charge order occurs in (TMTTF)<sub>2</sub>NO<sub>3</sub> [13, 18]. Like other salts with non-centrosymmetric anions, the salt undergoes a AO transition around 50 K, which was identified by X-ray diffraction and ESR measurements [15, 18]. Recent ESR data provided further evidence for the stabilization of a CO state below 250 K [19]. Here we present the results of detailed spectroscopic investigations of the charge distribution in (TMTTF)<sub>2</sub>NO<sub>3</sub> in the CO and AO states.

## II. MATERIALS AND EXPERIMENTS

The aciculate single crystals of (TMTTF)<sub>2</sub>NO<sub>3</sub> used for our investigations were grown by standard electrochemical methods [20]. The organic tetramethyltetratiofulvalene (TMTTF) donor molecules are stacked along the crystallographic  $a$ -axis; these stacks are separated by monovalent  $\text{NO}_3^-$  anions in the  $c$ -direction, as displayed in Fig. 1(a). In the normal state at ambient condition, the molecules are slightly dimerized along the chains with intra- and inter- dimer distances  $d_1$  and  $d_2$  respectively.

At elevated temperature, the planar  $\text{NO}_3^-$  anions exhibit orientational disorder with four possible arrangements for the nitrate ions, with each possible orientation rotated on  $30^\circ$  with respect to each other, as indicated in Fig. 1(c). Since there are in total twelve possible positions for oxygen, the anion almost resembles a nitrogen atom surrounded by an oxygen ring [21]. At reduced temperatures, below  $T_{\text{AO}}$ , the anions arrange in an or-

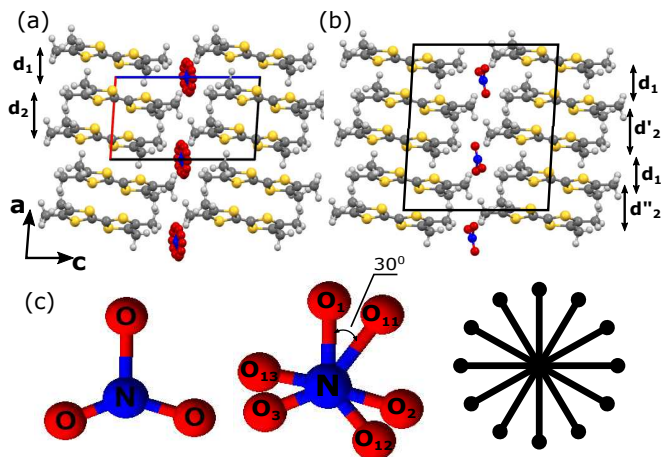


FIG. 1. (a) Crystal structure of  $(\text{TMTTF})_2\text{NO}_3$  where TMTTF stands for tetramethyltetrathiafulvalene at the normal state with finite dimerization and disordered anions,  $d_1$  and  $d_2$  are intra- and inter-dimers distances respectively. (b) Suggested low-temperature state with alternating orientation of the anions that leads to a doubling of the unit cell and tetramerization along the TMTTF molecular stack. (c) From the left to the right shape of the planar  $\text{NO}_3^-$  anion, the difference between two anion orientations, and all possible orientations are shown.

derly fashion. For the metallic analogue  $(\text{TMTSF})_2\text{NO}_3$ , which does not exhibit any ordering down to  $T_{\text{AO}} = 45$  K, the crystal structure in the anion-ordered state was resolved: here the anion order leads to a doubling of the unit cell [22, 23]. For  $(\text{TMTTF})_2\text{NO}_3$  we expect that the anion ordering leads to tetramerization of the TMTTF molecules with distances  $d_1, d'_2, d_1, d'_2$  as shown in Fig. 1(b).

In order to characterize the compound by dc resistivity measurements, two contacts were attached along the  $a$ -direction by carbon paste. To ensure good thermal contact, the samples were anchored to a sapphire plate and slowly cooled down to  $T = 20$  K. The voltage applied to the crystal was in the range of 0.5 to 5 V; from the measured current, the dc resistivity is calculated as a function of temperature,  $\rho(T)$ .

To learn about the charge disproportionation in  $(\text{TMTTF})_2\text{NO}_3$ , optical spectroscopy was performed utilizing a Bruker Hyperion infrared microscope attached to a Bruker Vertex 80v Fourier-transform infrared spectrometer. Reflectivity spectra  $R(\omega, T)$  were collected in a frequency range from 500 to 8000  $\text{cm}^{-1}$  between room temperature and 10 K. The optical conductivity  $\sigma(\omega)$  was calculated using Kramers-Kronig analysis with constant  $R(\omega)$  extrapolation below 500  $\text{cm}^{-1}$  and  $\omega^{-4}$  decay for higher frequencies. We first focused on the charge-sensitive infrared-active intramolecular vibrational mode  $\nu_{28}(\text{B}_{1u})$  [24]. These measurements were performed with the light polarized along the  $c$ -direction, i.e. perpendicular the main plane. As the amount of charge per TMTTF molecule is linearly related to the resonance frequency of

the  $\nu_{28}$  mode, charge imbalance in CO and AO states can be directly probed by tracking the peak positions upon cooling [10]. In addition, we performed reflection measurements off the crystal plane with the light polarized along the stacking direction (i.e.  $E \parallel a$ ).

We complemented our investigations by measurements of the electron spin resonance (ESR) down to low temperatures. The angular-dependence of the  $g$ -factor and linewidth  $\Delta H$  was obtained by a X-band spectrometer (Bruker EMXplus) as presented in detail in Ref. 19.

### III. RESULTS AND ANALYSIS

#### A. Transport properties

The solid black curve in Fig. 2(a) represents the temperature-dependent dc resistivity of  $(\text{TMTTF})_2\text{NO}_3$  measured along the  $a$ -axis; the overall behavior is reproduced on several single crystals. It is plotted in a double-logarithmic fashion to display the overall behavior. To identify the phase transitions more precisely, we

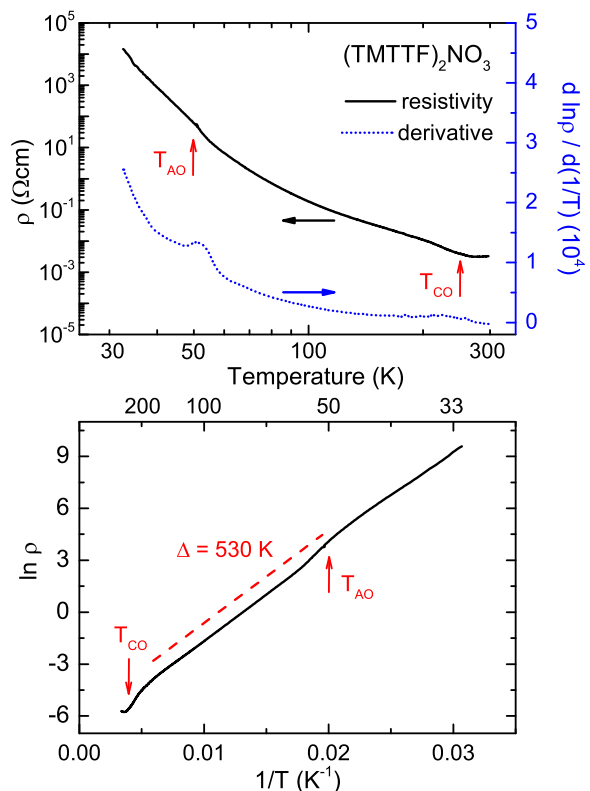


FIG. 2. Transport properties of  $(\text{TMTTF})_2\text{NO}_3$  along the chain direction  $a$ . (a) The black solid curve corresponds to the temperature dependence of the dc resistivity; note the double logarithmic scale on the left and bottom axis. The blue dotted curve gives the derivative  $d \ln \rho / d(1/T)$  corresponding to the linear right axis. (b) The Arrhenius plot of the temperature-dependent resistivity allows the extraction of an activation energy  $\Delta = 530$  K, indicated by the dashed red line.

calculate the derivative  $d\ln\rho/d(1/T)$  and plot it as a function of temperature by the dotted blue curve [16]. A most pronounced peak in  $d\ln\rho/d(1/T)$  is found at the AO transition around  $T_{AO} = 50$  K. The absence of any sign of hysteresis resembles more a second-order instead of a structure transition of first order. The broad minimum of  $\rho(T)$  at elevated temperature corresponds to the crossover from metal-like behavior to a charge-localized state; the zero-crossing in the derivative occurs at  $T_\rho \approx 280$  K, which is slightly higher than what was first reported by Coulon et al. [13] The CO transition temperature  $T_{CO} \approx 250$  K is also best identified in the local maximum in  $d\ln\rho/d(1/T)$ , which occurs when the resistivity exhibits a rapid increase around 225 K. Note, in  $(\text{TMTTF})_2\text{NO}_3$  salt the CO transition is more gradual compare to other Fabre salts because with decreasing anion size the interchain separation becomes smaller, and thus one-dimensionality is less pronounced [11, 25]. In Fig. 2(b) the Arrhenius plot of the resistivity is displayed, i.e.  $\ln\rho(T)$  versus inverse temperature  $1/T$ . The CO gap  $\Delta_{CO}$  can be extracted. The activated behavior continues with the same activation energy  $\Delta_{CO} \approx 530$  K below the AO transition.

## B. Magnetic properties

From our temperature dependent X-band ESR experiments we extract the intensity, resonance frequency and the line width [19]. Fig. 3(a) displays the ESR intensity  $I(T)$  normalized to the room temperature value  $I_{300\text{K}}$ , which corresponds to the spin susceptibility  $\chi_S(T)$ . The overall behaviour resembles the spin susceptibility of other  $(\text{TMTTF})_2X$  compounds [12, 26]. The intensity monotonically decreases upon cooling from room temperature to the anion-ordering transition at  $T_{AO} = 50$  K, below which the chain dimerizes accompanied by the formation of spin singlets, leading to the observed exponential decay of  $\chi_S(T)$  [14, 18, 26, 27]. The extracted spin gap  $\Delta_\sigma \approx 48$  K is similar for all three crystallographic directions and in agreement with previous reports [18].

At a first glance, the temperature dependence of the linewidth  $\Delta H(T)$  plotted in Fig. 3(b) exhibits no distinct features along any crystallographic axes; in fact, the behavior resembles the one known from  $(\text{TMTTF})_2\text{PF}_6$  where also no kink become obvious at  $T_{CO}$  [12]. A closer look, however, reveals that for the diagonal orientation a change in the slope for the derivative  $[d(\Delta H_{\text{diag}})/dT]$  occurs at  $T_{CO} = 250$  K, as indicated in the inset of Fig. 3. This observation is supported by the angular dependence of the ESR data reported in [19].

Here we plot the linewidth measured along the  $a$ -axis, the  $b$ -orientation as well as along  $45^\circ$ , i.e. between the  $a$ - and  $b$ -direction. Already around  $T = 250$  K the line of the diagonal-direction is broader than expected. At  $T \approx 125$  K the linewidth in the diagonal direction of the  $ab$ -plane becomes larger than along the  $a$ - and  $b$ -directions. This is taken as indication that a charge-order

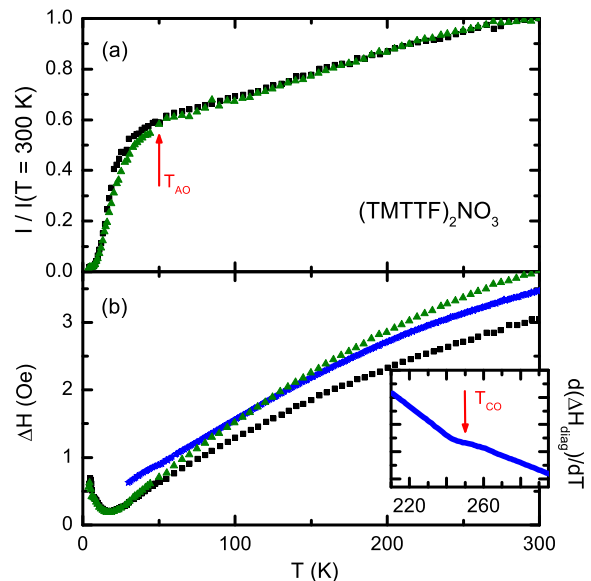


FIG. 3. ESR parameters of  $(\text{TMTTF})_2\text{NO}_3$  obtained from X-band measurements as a function of temperature. (a) The intensity  $I(T)$  for the  $a$ - and  $b$ -orientation normalized to the room temperature value. The ordering of the anions at  $T_{AO} = 50$  K causes a drop of the spin susceptibility. (b) The temperature dependent linewidth  $\Delta H$  measured along different directions:  $a$ -axis (black squares),  $b$ -direction (green triangles), and diagonal direction (blue stars). Strong evidence for the presence of charge order in this compound comes from the fact, that at  $T_{CO} = 250$  K the slope in the diagonal direction changes, as clearly shown in the inset, where the derivative of the smoothed data is plotted. This leads to a crossing (at around 125 K) of the temperature dependence for the linewidth obtained in the diagonal direction and the linewidth for the  $b$ -orientation.

transition is present in  $(\text{TMTTF})_2\text{NO}_3$ .

## C. Vibrational spectroscopy

Out of the molecular vibrations in TMTTF, three modes are most sensitive to the charge per molecule. Two of them are totally symmetric  $A_g$  ( $\nu_3$  and  $\nu_4$ ), and as a result they are infrared inactive; however they become visible via electron-molecular vibrational (emv) coupling [10]. The third one is an asymmetric infrared active  $B_{1u}$  ( $\nu_{28}$ ) mode which can be probed in out-of-plane direction (i.e.  $E \parallel c$ -axis). It exhibits a linear shift of the resonance frequency with ionicity of the TMTTF molecule due to the strengthening/loosening of the intramolecular bonds. The rather large intensity and weak coupling to the electronic background makes it ideal for investigation of the charge distribution. In the normal state, each TMTTF molecule contains the net charge  $\rho = +0.5e$ , which corresponds to one peak in the infrared spectra ( $\nu^{+0.5} = 1547 \text{ cm}^{-1}$ ).

In Fig. 4(a) the development of the  $\nu_{28}(B_{1u})$  mode

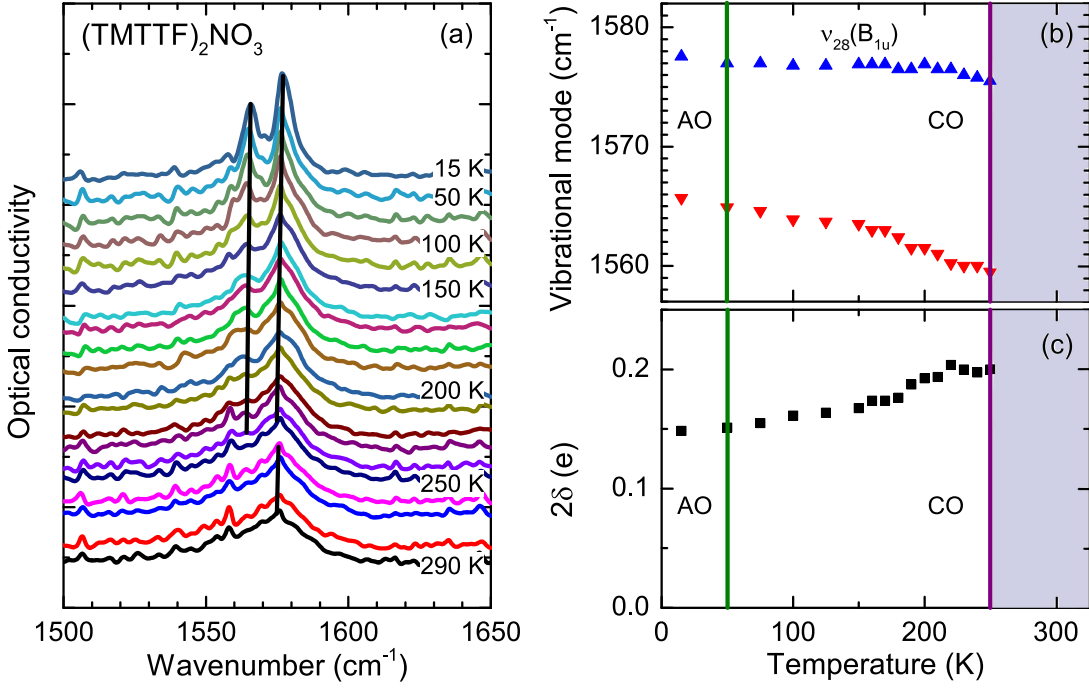


FIG. 4. (a) Temperature evolution of the charge-sensitive infrared-active molecular vibration  $\nu_{28}$  observed in the mid-infrared spectra of  $(\text{TMTTF})_2\text{NO}_3$  for  $E \parallel c$ . For clarity reasons, the curves are shifted with respect to each other. (b) Resonance frequency of the  $\nu_{28}(\text{B}_{1u})$  mode as a function of temperature obtained from fitting the spectra with two Lorentzians below  $T_{\text{CO}}$  (blue and red triangles). The peaks gradually diminish upon raising the temperature and cannot be reliably distinguished above  $T_{\text{CO}} = 250$  K. The grey area indicates that we present the fit results only below 250 K. The overall behavior resembles a gradual phase transition more than a rapid jump common to first-order transition. Note the slight upwards shift for  $T < T_{\text{AO}}$ . (c) By using Eq. (1) the charge imbalance  $2\delta$  can be directly calculated from the peak separation  $\Delta\nu$ .

is shown as the  $(\text{TMTTF})_2\text{NO}_3$  crystal is cooled down. While at room temperature we observe only one broad band that cannot be sensibly separated, two peaks are clearly distinguished below  $T = 250$  K. The  $\nu_{28}$  mode in  $(\text{TMTTF})_2\text{NO}_3$  is much broader compare to corresponding features observed in compounds with octahedral anions [10], and comparable to those seen for compounds with tetrahedral anions [17]. This can be attributed to the inherent disorder of the anions. To analyze the data qualitatively, we fit the  $\nu_{28}$  mode using two Lorentz oscillators, which works reasonably well up to  $T_{\text{CO}}$ . In Fig. 4(b) the resonance frequencies are depicted as a function of temperature. Due to the increasing line width and diminishing intensity, it was not possible to reliably separate two contributions above 250 K, as illustrated in Fig. 5. The absence of a sensible fit results is indicated by the shaded area. Note, that this is a gradual process resembling a continuous second-order phase transition. In addition, we can identify a simultaneous upshift of both modes by less than  $1 \text{ cm}^{-1}$  as the AO state is entered below 50 K; also the intensity of the modes increases. From the positions of the two peaks, the charge imbalance  $2\delta$  can be calculated via

$$2\delta = \frac{\Delta\nu}{80 \text{ cm}^{-1}}, \quad (1)$$

where  $\Delta\nu$  is the spectral separation between the peaks

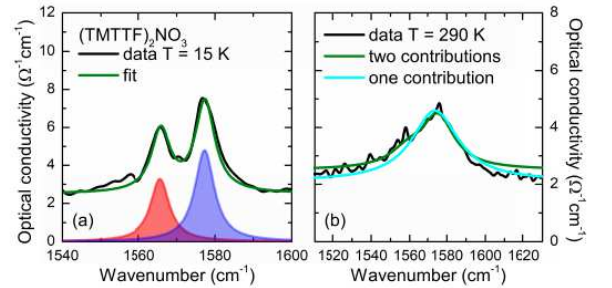


FIG. 5. Vibrational spectra of  $(\text{TMTTF})_2\text{NO}_3$  in the range of the  $\nu_{28}$  mode. (a) The 15 K spectrum can be readily fitted with two Lorentzians, indicated by the red and blue curves; the overall fit is represented by the green line. (b) At  $T = 290$  K the curve is much broader (note, the frequency scale differs by a factor of 2) and the mode less pronounced. We present a fit of the data with one contribution (cyan line) and two contributions (green line) and conclude that a two-component fit is not sensible.

in the CO state.

The temperature dependence of  $2\delta(T)$  is plotted as a function of temperature in Fig. 4(c). It becomes obvious at  $T_{\text{CO}} = 250$  K and reaches the maximum  $2\delta = (0.21 \pm 0.01)e$  at 220 K; this perfectly matches the temperatures

obtained from the transport data [Fig. 2(a)]. The charge disproportionation then gradually decreases to  $0.15e$ , and remains unchanged in the AO state.

## IV. DISCUSSION

### A. Charge order transition

In the case of Fabre salts with highly symmetric anions, such as  $(\text{TMTTF})_2\text{SbF}_6$  and  $(\text{TMTTF})_2\text{AsF}_6$ , a noticeable kink in the ESR linewidth has been identified at  $T_{\text{CO}}$  [12]. The charge disproportionation on the TMTTF molecules leads to nonequivalent couplings between the anions and the TMTTF molecules that influences the magnetic behavior of the spin chain. The ESR linewidth of  $(\text{TMTTF})_2\text{NO}_3$ , however, barely changes at  $T_{\text{CO}}$ ; only a plateau in the derivative is identified in the inset of Fig. 3.

The low-temperatures optical spectra of  $(\text{TMTTF})_2\text{NO}_3$  displayed in Fig. 4(a) contain two vibrational features corresponding to  $\nu_{28}$  that reflect the presence of two TMTTF sites containing non-equivalent charge; the strength of the low-frequency feature gradually diminishes upon warming up, can barely be resolved above 200 K and becomes undistinguishable around  $T_{\text{CO}}$ . Traces of charge disproportionation might be already present at room temperature, as observed in some BEDT-TTF compounds [28, 29], for instance; however, the width of the vibrational band and the weakness of the second feature does not allow a firm conclusion. Beyond this uncertainty,  $2\delta(T)$  continuously decreases when cooling below  $T_{\text{CO}}$  before it saturates around  $0.15e$ , as depicted in Fig. 4(c). It stays almost the same in the AO state, and we can conclude that the effect of the AO on charge distribution is rather small.

From a comparative study [17] Pustogov *et al.* concluded that the CO state in  $(\text{TMTTF})_2X$  salts with octahedral and tetrahedral anions is determined by the stacking of the organic molecules and independent on symmetry of the anions. In other words, the CO state is only governed by the competition between intersite Coulomb repulsion  $V$  on the one hand and overlap integral  $t$  or bandwidth  $W$  on the other hand. In first approximation, the charge imbalance  $2\delta$  should be proportional to the charge gap  $\Delta_{\text{CO}}$  and to the effective correlations  $V/W$ . In the corresponding plot, Fig. 6, we illustrate that  $(\text{TMTTF})_2\text{NO}_3$  nicely follows the linear dependence between  $2\delta$  obtained from vibrational spectroscopy and  $\Delta_{\text{CO}}$  extracted from the transport measurements. This observation suggests that the CO state is mainly driven by Coulomb repulsion that occurs from charge imbalance between neighboring sites in the organic stack. Here the anion potential seems to play only a minor role. Interestingly,  $(\text{TMTTF})_2\text{NO}_3$  does not follow the general relation between  $T_{\text{CO}}$  and  $2\delta$  [17]; as a matter is fact, the charge order transition occurs at about twice the temperature as expected.

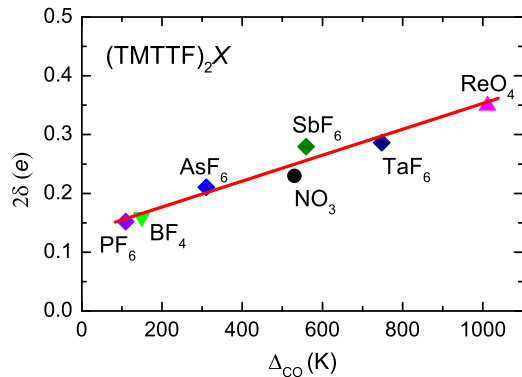


FIG. 6. Amount of charge disproportionation  $2\delta$  plotted versus the charge-order gap  $\Delta_{\text{CO}}$  obtained from temperature-dependent transport measurements [8, 11]. The red line indicates the linear dependence between  $2\delta$  and  $\Delta_{\text{CO}}$ .

### B. Anion order

At elevated temperatures the anions of Fabre salts are randomly oriented; due to entropy reasons the non-centrosymmetric anions prefer to become oriented upon cooling. The increasing charge disproportionation on the TMTTF stacks below  $T_{\text{CO}}$  and their coupling to the anions, however, is not sufficient to completely order the anions. From our dc resistivity measurements (Fig. 2) we see that the AO transition takes place only at  $T_{\text{AO}} = 47$  K, in coarse agreement with previous results [13, 14]. Although this is a structural transition, we do not observe a hysteresis in the resistivity data, in good agreement with previous results [30, 31]. The small size of the  $\text{NO}_3^-$  anion might be one reason why the phase transition inclines towards second order. This also implies a weak coupling to the TMTTF molecules and minor influence on the electronic properties of  $(\text{TMTTF})_2\text{NO}_3$ , as seen in the insignificant change of the resistivity below  $T_{\text{AO}} = 47$  K.

The particular shape and the small size of the  $\text{NO}_3^-$  anions explain, why the  $T_{\text{AO}}$  is far below the transition temperature observed in  $(\text{TMTTF})_2\text{ReO}_4$  (157K) and  $(\text{TMTTF})_2\text{ClO}_4$  (73.4K) which contain much large anions. The other Fabre salt with tetrahedral anion,  $(\text{TMTTF})_2\text{BF}_4$ , seems to make an exception, with  $T_{\text{AO}} = 41.5$  K. For tetrahedral anions, sulfur-ligand interactions govern the charge distribution in the AO state, while for  $(\text{TMTTF})_2\text{NO}_3$   $-\text{CH}_3 \cdots \text{O}$  interactions are more important; we will come back to this in the subsequent Section IV C. In the case of the planar  $\text{NO}_3^-$  anions, the three-dimensional rotation of the entire molecule might be frozen at much higher temperatures – for instance at  $T_{\text{CO}}$  – while rotation within the plane continues down to  $T_{\text{AO}}$ .

It is interesting to note that both branches of the  $\nu_{28}(A_g)$  vibrational mode reveals a slight upshift at  $T_{\text{AO}}$ , as seen in Fig. 4(b). This could indicate a minute reduction in the overall charge transfer. Or it indicates a

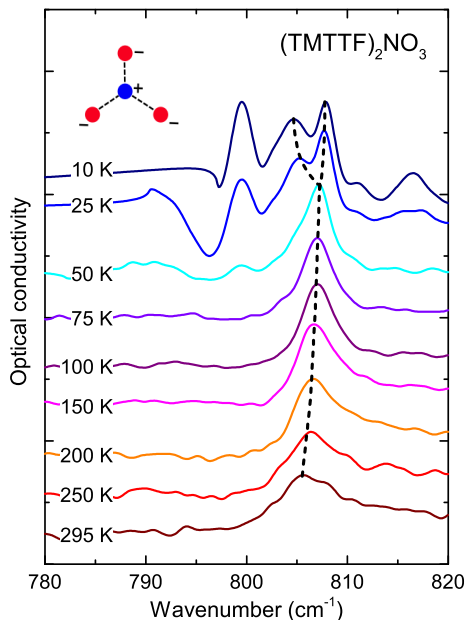


FIG. 7. Temperature evolution of the optical conductivity in the region of the fundamental  $\nu_2$  mode of  $\text{NO}_3^-$  anion measured for  $E \parallel c$ -axis. The curves are displaced for clarity. The dashed black line tracks the resonance frequency of the  $\nu_2$  molecular vibration upon cooling and visualizes the splitting below  $T_{\text{AO}} = 50$  K.

general stiffening of the vibrational pattern due to interaction with the anion, which move closer to the TMTTF molecules.

A deeper insight into the anion ordering is gained by looking at the vibrations of the  $\text{NO}_3^-$  anions. the out-of-plane bending mode  $\nu_2$  shows up rather prominently around  $810 - 820 \text{ cm}^{-1}$  [32, 33]. From the temperature dependence of this fundamental mode plotted in Fig. 7, we observe a clear splitting below  $T_{\text{AO}} = 50$  K. This could simply be explained by a distortion of the  $\text{NO}_3^-$  anions at the transition resulting in breaking of the triangular symmetry. But we can also imagine different amounts of charge on the anions in their ordered state; in other words, the anion order causes some charge order in the  $\text{NO}_3^-$  chain. This is a result of the alternating coupling to the TMTTF molecules, leading to a tetramerization there.

### C. Tetramerization

The  $(\text{TMTTF})_2X$  stoichiometry already imposes a dimerization onto the TMTTF stacks, as depicted in Fig. 1(a). The AO with a wavevector  $(\frac{1}{2}, 0, 0)$  leads to a tetramerization in the  $(\text{TMTTF})_2\text{NO}_3$  salt, i.e. a doubling of the unit cell along the  $a$ -axis [Fig. 1(b)]. Importantly, this is not just a structural order due the alternating orientation of the anions but also a shift of the anions within the methyl-group cavity. Furthermore

it affects the link towards the S atom and rearranges the charges [17, 34]. Due to the small size and minor shift of the  $\text{NO}_3^-$  anions, this structural alternation is quite weak compared to other  $(\text{TMTTF})_2X$  salts, nevertheless it is a crucial phenomenon even in the present case. For the sister compound  $(\text{TMTSF})_2\text{NO}_3$  – where sulfur atoms are substituted by Se – the AO transition is very similar and the wavevector is identical. It was shown for this compound [35] that the  $-\text{CH}_3 \cdots \text{O}$  interactions are important; the anion reorientation below  $T_{\text{AO}}$  and the shift toward selected methyl groups cause a change of the charge pattern, where donors with shorter  $-\text{CH}_3 \cdots \text{O}$  distances are more positively charged (charge rich), while donors with smaller  $-\text{CH}_3 \cdots \text{O}$  distances are charge poor [22, 23, 36]. We do expect a similar behavior for  $(\text{TMTTF})_2\text{NO}_3$ : the uniform charge distribution at elevated temperatures becomes alternated below  $T_{\text{CO}}$  presumably by the nearest-neighbor Coulomb repulsion  $V$ . In a second step, this 1010 alternation will change to a 0110 pattern in the AO state, as depicted in Fig. 8.

This corresponds exactly to the charge disproportionation within the  $\text{NO}_3^-$  anions, inferred from Fig. 7: below  $T_{\text{AO}}$  the fundamental vibrational modes splits because every second anion becomes charge rich while the other are depleted.

An unambiguous proof of the tetramerization along the stacks is given in Fig. 9, where the appearance of the  $\nu_4(A_g)$  vibration of the TMTTF molecule is observed as  $T < T_{\text{AO}}$ . This fully symmetric mode is typically seen in Raman spectroscopy but infrared silent [10], however, an out-of-phase coupling can make them infrared active. In the present case, AO activates the dimeric in-phase vibration by out-of-phase combination of two dimers within the tetramer; the  $\nu_{4,\text{gu}}$  mode couples to infrared light via the a dipole between the dimers [17]. In Fig. 9 we see this feature at around  $1410 \text{ cm}^{-1}$  appearing in the  $E \parallel a$  spectra below 50 K. Compare to other Fabre salts with

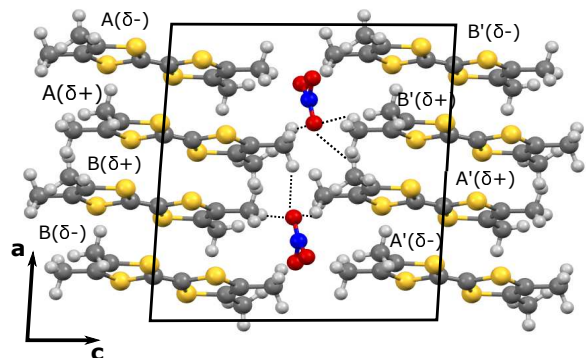


FIG. 8. Sketch of the  $(\text{TMTTF})_2\text{NO}_3$  tetramer in the charge and anion ordered state at low temperatures. Here the dimers A and A', as well as B and B' are linked via inversion symmetry. The dashed lines indicate the shortest  $-\text{CH}_3 \cdots \text{O}$  distances.  $(\delta^+)$  corresponds to the charge rich sites and  $(\delta^-)$  to the charge poor ones; forming a 0110 pattern along the  $a$ -direction.

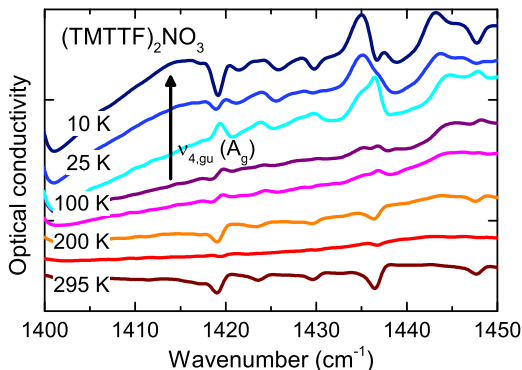


FIG. 9. Temperature dependence of the mid-infrared spectra of  $(\text{TMTTF})_2\text{NO}_3$  probed with  $E \parallel a$ . Around 1410 to 1420  $\text{cm}^{-1}$  the  $\nu_{4,gu}(A_g)$  mode becomes activated by the tetramerization in the AO state.

non-centrosymmetric anions, the intensity of this mode is relatively small; but this is consistent with the fact that tetramerization in  $(\text{TMTTF})_2\text{NO}_3$  is rather weak. With growing anion size  $d(\text{NO}_3) < d(\text{BF}_4) < d(\text{ClO}_4) < d(\text{ReO}_4)$  the tetramerization is more pronounced and the intensity of the  $\nu_{4,gu}$  mode increases. This supports the assumption that the 0110 charge arrangement in the AO state is mainly due to the anionic potential and anion arrangement; while the CO state is governed by nearest-neighbor Coulomb repulsion.

In Fig. 2 we have demonstrated that the anion-ordering transition affects the transport properties as a slight kink at  $T_{\text{AO}}$ , but does not lead to drastic step with a hysteretic behavior. The activation energy remains unchanged, only some offset is observed; in other words, the physical state above  $T_{\text{AO}}$  is very similar to the low-temperature phase. The tetramerization on the TMTTF stack is most prominent in ESR properties [13, 14, 19]

where spin singlets are formed below  $T_{\text{AO}}$  leading to an exponential decay of the spin susceptibility as presented in Fig. 3. From the corresponding fit we obtain a spin gap  $\Delta_\sigma \approx 48$  K in full accord with previous observations. It is interesting to note that the phase transition occurs much more gradual, compared to  $(\text{TMTTF})_2\text{BF}_4$  or  $(\text{TMTTF})_2\text{ReO}_4$  [12], for instance.

## V. CONCLUSIONS

Detailed transport, ESR and infrared studies on  $(\text{TMTTF})_2\text{NO}_3$  were performed to explore the charge-ordered and anion-ordered states in this salt. From the different methods we independently determine the charge order transition at  $T_{\text{CO}} \approx 250$  K with a charge imbalance of  $2\delta = 0.2e$ . Our findings suggest that the charge disproportionation in the CO state is mainly governed by intersite Coulomb repulsion and solely determined by the TMTTF stacks. The universal dependence between the charge imbalance  $2\delta$  and size of the CO gap  $\Delta_{\text{CO}}$  also holds for  $(\text{TMTTF})_2\text{NO}_3$ . In the AO state the  $\text{NO}_3^-$  anions order in an alternating fashion. Due to the  $-\text{CH}_3 \cdots \text{O}$  interaction charge pattern changes towards 0110 below  $T_{\text{AO}} = 50$  K. This not only causes a step in the dc resistivity, but most prominent the formation of spin singlets, leading to an exponential drop in the spin susceptibility.

## VI. ACKNOWLEDGEMENTS

We acknowledge the support by the Deutsche Forschungsgemeinschaft and appreciate helpful discussions with A. Pustogow.

- 
- [1] T. Giamarchi, *Quantum Physics in One Dimension* (Oxford University Press, Oxford, 2004).
- [2] D. Baeriswyl and L. Degiorgi, eds., *Strong Interactions In Low Dimensions*, Physics and chemistry of materials with low-dimensional structures, Vol. 25 (Kluwer Academic, Dordrecht, 2004).
- [3] D. Jérôme and H. J. Schulz, Organic conductors and superconductors, *Advances in Physics* **31**, 299 (1982).
- [4] J.-P. Farges, *Organic conductors: fundamentals and applications* (Marcel Dekker, 1994).
- [5] M. Dressel, Spin-charge separation in quasi one-dimensional organic conductors, *Naturwissenschaften* **90**, 337 (2003); Ordering phenomena in quasi-one-dimensional organic conductors, *Naturwissenschaften* **94**, 527 (2007).
- [6] S. Tomić and M. Dressel, Ferroelectricity in molecular solids: a review of electrodynamic properties, *Reports on Progress in Physics* **78**, 096501 (2015).
- [7] J.-P. Pouget, P. Alemany, and E. Canadell, Donor-anion interactions in quarter-filled low-dimensional organic conductors, *Materials Horizons* **5**, 590 (2018); M. Dressel and S. Tomić, Molecular quantum materials: electronic phases and charge dynamics in two-dimensional organic solids, *Advances in Physics* **69**, 1 (2020).
- [8] D. S. Chow, F. Zamborszky, B. Alavi, D. J. Tantillo, A. Baur, C. A. Merlic, and S. E. Brown, Charge ordering in the TMTTF family of molecular conductors, *Phys. Rev. Lett.* **85**, 1698 (2000); F. Zamborszky, W. Yu, W. Raas, S. E. Brown, B. Alavi, C. A. Merlic, and A. Baur, Competition and coexistence of bond and charge orders in  $(\text{TMTTF})_2\text{AsF}_6$ , *Phys. Rev. B* **66**, 081103 (2002); W. Yu, F. Zhang, F. Zamborszky, B. Alavi, A. Baur, C. A. Merlic, and S. E. Brown, Electron-lattice coupling and broken symmetries of the molecular salt  $(\text{TMTTF})_2\text{SbF}_6$ , *Phys. Rev. B* **70**, 121101 (2004).
- [9] P. Monceau, F. Y. Nad, and S. Brazovskii, Ferroelectric mott-hubbard phase of organic  $(\text{TMTTF})_2\text{X}$  conductors, *Phys. Rev. Lett.* **86**, 4080 (2001); F. Nad and P. Monceau, Dielectric response of the charge or-

- dered state in quasi-one-dimensional organic conductors, *Journal of the Physical Society of Japan* **75**, 051005 (2006); P. Monceau, Electronic crystals: an experimental overview, *Advances in Physics* **61**, 325 (2012).
- [10] M. Dumm, B. Salameh, M. Abaker, L. K. Montgomery, and M. Dressel, Magnetic and optical studies of spin and charge ordering in  $(\text{TMTTF})_2\text{AsF}_6$ , *J. Phys. IV France* **114**, 57 (2004); M. Dumm, M. Abaker, and M. Dressel, Mid-infrared response of charge-ordered quasi-1d organic conductors  $(\text{TMTTF})_2\text{X}$ , *J. Phys. IV France* **131**, 55 (2005); M. Dressel, M. Dumm, T. Knoblauch, and M. Masino, Comprehensive optical investigations of charge order in organic chain compounds  $(\text{TMTTF})_2\text{X}$ , *Crystals* **2**, 528 (2012).
- [11] Y. Oka, N. Matsunaga, K. Nomura, A. Kawamoto, K. Yamamoto, and K. Yakushi, Charge order in  $(\text{tmTF})_2\text{taf}_6$  by infrared spectroscopy, *Journal of the Physical Society of Japan* **84**, 114709 (2015).
- [12] T. Nakamura, Possible charge ordering patterns of the paramagnetic insulating states in  $(\text{TMTTF})_2\text{X}$ , *Journal of the Physical Society of Japan* **72**, 213 (2003); K. Furukawa, T. Hara, and T. Nakamura, Deuteration effect and possible origin of the charge-ordering transition of  $(\text{TMTTF})_2\text{X}$ , *Journal of the Physical Society of Japan* **74**, 3288 (2005); Y. Nogami, T. Ito, K. Yamamoto, N. Irie, S. Horita, T. Kambe, N. Nagao, K. Oshima, N. Ikeda, and T. Nakamura, X-ray structural study of charge and anion orderings of TMTTF salts, *J. Phys. IV France* **131**, 39 (2005); F. Iwase, K. Sugiura, K. Furukawa, and T. Nakamura,  $^{13}\text{C}$  NMR of the magnetic properties of the quasi-one-dimensional conductor  $(\text{TMTTF})_2\text{SbF}_6$ , *Phys. Rev. B* **84**, 115140 (2011); B. Salameh, S. Yasin, M. Dumm, G. Untereiner, L. Montgomery, and M. Dressel, Spin dynamics of the organic linear chain compounds  $(\text{TMTTF})_2\text{X}$  ( $\text{X}=\text{SbF}_6, \text{AsF}_6, \text{BF}_4, \text{ReO}_4$ , and  $\text{SCN}$ ), *Phys. Rev. B* **83**, 205126 (2011); S. Yasin, B. Salameh, E. Rose, M. Dumm, H.-A. Krug von Nidda, A. Loidl, M. Ozerov, G. Untereiner, L. Montgomery, and M. Dressel, Broken magnetic symmetry due to charge-order ferroelectricity discovered in  $(\text{TMTTF})_2\text{X}$  salts by multifrequency ESR, *Phys. Rev. B* **85**, 144428 (2012); M. Dressel, M. Dumm, T. Knoblauch, B. Köhler, B. Salameh, and S. Yasin, Charge order breaks magnetic symmetry in molecular quantum spin chains, *Advances in Condensed Matter Physics* **2012**, 398721 (2012).
- [13] C. Coulon, P. Delhaes, S. Flandrois, R. Lagnier, E. Bonjour, and J. M. Fabre, A new survey of the physical properties of the  $(\text{TMTTF})_2\text{X}$  series. role of the counterion ordering, *J. Phys. France* **43**, 1059 (1982).
- [14] R. Moret, J. P. Pouget, R. Comès, and K. Bechgaard, Structural phase transitions in the  $(\text{TMTSF})_2\text{X}$  and  $(\text{TMTTF})_2\text{X}$  series : A survey with some new results, *J. Phys. Colloques* **44**, C3 (1983).
- [15] J. P. Pouget, R. Moret, R. Comes, K. Bechgaard, J. M. Fabre, and L. Giral, X-ray diffuse scattering study of some  $(\text{TMTSF})_2\text{X}$  and  $(\text{TMTTF})_2\text{X}$  salts, *Molecular Crystals and Liquid Crystals* **79**, 485 (1982); S. Ravy, R. Moret, J. P. Pouget, and R. Comes, Structural phase transitions in  $(\text{TMTSF})_2\text{X}$  and related compounds, *Synthetic Metals* **13**, 63 (1986).
- [16] R. Rösslhuber, E. Rose, T. Ivek, A. Pustogow, T. Breier, M. Geiger, K. Schrem, G. Untereiner, and M. Dressel, Structural and electronic properties of  $(\text{TMTTF})_2\text{X}$  salts with tetrahedral anions, *Crystals* **8**, 10.3390/cryst8030121 (2018).
- [17] A. Pustogow, T. Peterseim, S. Kolatschek, L. Engel, and M. Dressel, Electronic correlations versus lattice interactions: Interplay of charge and anion orders in  $(\text{TMTTF})_2\text{X}$ , *Phys. Rev. B* **94**, 195125 (2016).
- [18] C. Coulon, P. Foury-Leylekian, J.-M. Fabre, and J.-P. Pouget, Electronic instabilities and irradiation effects in the  $(\text{TMTTF})_2\text{X}$  series, *The European Physical Journal B* **88**, 85 (2015).
- [19] L. N. Majer, B. Miksch, G. G. Lesseux, G. Untereiner, and M. Dressel, Charge-order phase transition in the quasi one-dimensional organic conductor  $(\text{TMTTF})_2\text{NO}_3$ , *Appl. Magn. Res.* **51**, 1321 (2020).
- [20] B. Köhler, E. Rose, M. Dumm, G. Untereiner, and M. Dressel, Comprehensive transport study of anisotropy and ordering phenomena in quasi-one-dimensional  $(\text{TMTTF})_2\text{X}$  salts ( $\text{X}=\text{PF}_6, \text{AsF}_6, \text{SbF}_6, \text{BF}_4, \text{ClO}_4, \text{ReO}_4$ ), *Phys. Rev. B* **84**, 035124 (2011).
- [21] B. Liautard, S. Peytavin, G. Brun, and M. Maurin, Etude structurale du nitrate de tétraméthyltétrathiafulvalène  $(\text{TMTTF})_2\text{NO}_3$ , *Acta Crystallographica Section B* **38**, 2746 (1982).
- [22] Y. Barrans, J. Gaultier, S. Bracchetti, P. Guionneau, D. Chasseau, and J. M. Fabre, Low temperature structural properties of the  $(\text{TMTSF})_2\text{NO}_3$  salt, *Synthetic Metals* **103**, 2042 (1999).
- [23] B. Guster, M. Pruneda, P. Ordejón, E. Canadell, and J.-P. Pouget, Anion ordering transition and fermi surface electron-hole instabilities in the  $(\text{TMTSF})_2\text{ClO}_4$  and  $(\text{TMTSF})_2\text{NO}_3$  bechgaard salts analyzed through the first-principles lindhard response function, *Journal of Physics: Condensed Matter* **33**, 085705 (2020).
- [24] M. Meneghetti, R. Bozio, I. Zanon, C. Pecile, C. Ricotta, and M. Zanetti, Vibrational behavior of molecular constituents of organic superconductors: TMTSF, its radical cation and the sulphur analogs TMTTF and  $\text{TMTSF}^+$ , *The Journal of Chemical Physics* **80**, 6210 (1984).
- [25] T. Knoblauch and M. Dressel, Charge disproportionation in  $(\text{TMTTF})_2\text{X}$  ( $\text{X}=\text{PF}_6, \text{AsF}_6$  and  $\text{SbF}_6$ ) investigated by infrared spectroscopy, *physica status solidi c* **9**, 1158 (2012).
- [26] M. Dumm, A. Loidl, B. W. Fravel, K. P. Starkey, L. K. Montgomery, and M. Dressel, Electron spin resonance studies on the organic linear-chain compounds  $(\text{TMTcF})_2x$  ( $c = \text{S, Se}$ ;  $x=\text{PF}_6, \text{AsF}_6, \text{ClO}_4, \text{Br}$ ), *Phys. Rev. B* **61**, 511 (2000).
- [27] M. Dumm, A. Loidl, B. Alavi, K. P. Starkey, L. K. Montgomery, and M. Dressel, Comprehensive esr study of the antiferromagnetic ground states in the one-dimensional spin systems  $(\text{TMTSF})_2\text{PF}_6$ ,  $\text{TMTSF}_2\text{AsF}_6$ , and  $(\text{TMTTF})_2\text{Br}$ , *Phys. Rev. B* **62**, 6512 (2000).
- [28] T. Ivek, B. Korin-Hamzić, O. Milat, S. Tomić, C. Clauss, N. Drichko, D. Schweitzer, and M. Dressel, Electrodynamic response of the charge ordering phase: Dielectric and optical studies of  $\alpha$ - $(\text{BEDT-TTF})_2\text{I}_3$ , *Phys. Rev. B* **83**, 165128 (2011).
- [29] A. Pustogow, Y. Saito, A. Rohwer, J. A. Schlueter, and M. Dressel, Coexistence of charge order and superconductivity in  $\beta''$ - $(\text{BEDT-TTF})_2\text{SF}_5\text{CH}_2\text{CF}_2\text{SO}_3$ ,



- [Phys. Rev. B \*\*99\*\*, 140509 \(2019\)](#); A. Pustogow, K. Trepow, A. Rohwer, Y. Saito, M. Sanz Alonso, A. Löhle, J. A. Schlueter, and M. Dressel, Charge order in  $\beta''$ -phase bedt-ttf salts, [Phys. Rev. B \*\*99\*\*, 155144 \(2019\)](#).
- [30] J. Pouget and S. Ravy, Structural Aspects of the Bechgaard Salts and Related Compounds, [Journal de Physique I \*\*6\*\*, 1501 \(1996\)](#).
- [31] J.-P. Pouget, Structural aspects of the bechgaard and fabre salts: An update, [Crystals \*\*2\*\*, 466 \(2012\)](#).
- [32] J. L. Stewart, The infrared spectrum of the nitrate ion in various crystalline environments, (1964).
- [33] J.-P. Mathieu and M. Lounsbury, The raman spectra of metallic nitrates and the structure of concentrated solutions of electrolytes, [Discussions of the Faraday Society \*\*9\*\*, 196 \(1950\)](#).
- [34] D. Le Pévelin, J. Gaultier, Y. Barrans, D. Chasseau, F. Castet, and L. Ducasse, Temperature and pressure dependencies of the crystal structure of the organic superconductor  $(\text{TMTSF})_2\text{ClO}_4$ , [The European Physical Journal B - Condensed Matter and Complex Systems \*\*11\*\*, 103 \(1998\)](#).
- [35] T. J. Emge, M. A. Beno, C. A. Daws, H. H. Wang, and J. M. Williams, Novel structural features, and their relationship to the electrical properties, of the organic conductor  $(\text{TMTSF})_2\text{NO}_3$  at 298 K and 125 K, [Molecular Crystals and Liquid Crystals \*\*116\*\*, 153 \(1984\)](#).
- [36] P. Alemany, J.-P. Pouget, and E. Canadell, Electronic structure and anion ordering in  $(\text{TMTSF})_2\text{ClO}_4$  and  $(\text{TMTSF})_2\text{NO}_3$ : A first-principles study, [Phys. Rev. B \*\*89\*\*, 155124 \(2014\)](#).